Copper Metabolism Domain-Containing 1 Represses Genes That Promote Inflammation and Protects Mice From Colitis and Colitis-Associated Cancer

Li, Haiying; Chan, Lillienne; Bartuzi, Paulina; Melton, Shelby D.; Weber, Axel; Ben-Shlomo, Shani; Varol, Chen; Raetz, Megan; Mao, Xicheng; Starokadomskyy, Petro

Published in:
Gastroenterology

DOI:
10.1053/j.gastro.2014.04.007

Publication date:
2014

Gastroenterology 2014;147:184–195

Copper Metabolism Domain-Containing 1 Represses Genes That Promote Inflammation and Protects Mice From Colitis and Colitis-Associated Cancer

Haiying Li,[1] Lillienne Chan,[1] Paulina Bartuzi,[2] Shelby D. Melton,[3] Axel Weber,[4] Shani Ben–Shlomo,[5] Chen Varol,[5] Megan Raetz,[6] Xicheng Mao,[1] Petro Starokadomskyy,[1] Suzanne van Sommeren,[7] Mohamad Mokadem,[1] Heike Schneider,[8] Reid Weisberg,[1] Harm-Jan Westra,[9] Tõnu Esko,[10] Andres Metspalu,[10] Vinod Kumar,[9] William A. Faubion,[11] Felix Yarovinsky,[6] Marten Hofker,[2] Cisca Wijmenga,[9] Michael Kracht,[4] Lude Franke,[9] Vincent Aguirre,[1] Rinse K. Weersma,[7] Nathan Gluck,[5] Bart van de Sluis,[2] and Ezra Burstein[1,12]

[1]Department of Internal Medicine, [6]Department of Immunology, and [12]Department of Molecular Biology, University of Texas Southwestern Medical Center, Dallas, Texas; [2]Department of Pediatrics (Section of Molecular Genetics), [9]Department of Genetics, and [7]Department of Gastroenterology and Hepatology, University of Groningen, University Medical Center Groningen, Groningen, The Netherlands; [3]Department of Pathology, Dallas VA Medical Center, Dallas, Texas; [4]Rudolf Buchheim Institute of Pharmacology, Justus Liebig University, Giessen, Germany; [5]Gastroenterology Institute, Tel Aviv Sourasky Medical Center, Tel Aviv, Israel; [10]Estonian Genome Center, University of Tartu, Tartu, Estonia; [11]Division of Gastroenterology and Hepatology, Mayo Clinic, Rochester, Minnesota; and [8]Institute of Physiological Chemistry, Hannover Medical School, Hannover, Germany

BACKGROUND & AIMS: Activation of the transcription factor nuclear factor-κB (NF-κB) has been associated with the development of inflammatory bowel disease (IBD). Copper metabolism MURR1 domain containing 1 (COMMD1), a regulator of various transport pathways, has been shown to limit NF-κB activation. We investigated the roles of COMMD1 in the pathogenesis of colitis in mice and IBD in human beings. **METHODS:** We created mice with a specific disruption of *Commd1* in myeloid cells (Mye-knockout [K/O] mice); we analyzed immune cell populations and functions and expression of genes regulated by NF-κB. Sepsis was induced in Mye-K/O and wild-type mice by cecal ligation and puncture or intraperitoneal injection of lipopolysaccharide (LPS), colitis was induced by administration of dextran sodium sulfate, and colitis-associated cancer was induced by administration of dextran sodium sulfate and azoxymethane. We measured levels of *COMMD1* messenger RNA in colon biopsy specimens from 29 patients with IBD and 16 patients without (controls), and validated findings in an independent cohort (17 patients with IBD and 22 controls). We searched for polymorphisms in or near *COMMD1* that were associated with IBD using data from the International IBD Genetics Consortium and performed quantitative trait locus analysis. **RESULTS:** In comparing gene expression patterns between myeloid cells from Mye-K/O and wild-type mice, we found that COMMD1 represses expression of genes induced by LPS. Mye-K/O mice had more intense inflammatory responses to LPS and developed more severe sepsis and colitis, with greater mortality. More Mye-K/O mice with colitis developed colon dysplasia and tumors than wild-type mice. We observed a reduced expression of COMMD1 in colon biopsy specimens and circulating leukocytes from patients with IBD. We associated single-nucleotide variants near *COMMD1* with reduced expression of the gene and linked them with increased risk for ulcerative colitis. **CONCLUSIONS:** Expression of COMMD1 by myeloid cells has anti-inflammatory effects. Reduced expression or function of COMMD1 could be involved in the pathogenesis of IBD.

Keywords: Mouse Model; Gene Regulation; CD; UC.

BASIC AND TRANSLATIONAL AT

Persistent inflammation is a common maladaptive component in the pathogenesis of human diseases. A prime example of this paradigm is inflammatory bowel disease (IBD), a chronic inflammatory process of the intestinal tract that clinically presents as 2 phenotypic entities: ulcerative colitis (UC) and Crohn's disease (CD). This disorder involves an interaction between environmental factors and inherited susceptibility, and is associated with an increased risk for colorectal cancer.[1]

The regulation of the inflammatory cascade is a complex process in which the transcription factor nuclear factor-κB (NF-κB) plays a master regulatory role.[2] Consequently, this factor also has been linked to the pathogenesis of several chronic inflammatory conditions in human beings,[2] including IBD.[3,4] Canonical NF-κB activity is mediated

Abbreviations used in this paper: **BMDM, bone marrow–derived myeloid cells; CD, Crohn's disease; *cis*-eQTL, *cis*-expression quantitative trait locus; COMMD1, copper metabolism MURR1 domain containing 1; DSS, dextran sodium sulfate; IBD, inflammatory bowel disease; IIBDGC, International IBD Genetic Consortium; Il, interleukin; KEGG, Kyoto encyclopedia of genes and genomes; K/O, knockout; LPS, lipopolysaccharide; mRNA, messenger RNA; Mye-K/O, myeloid-specific Commd1 knockout; NF-κB, nuclear factor-κB; SNP, single-nucleotide polymorphism; Tnf, tumor necrosis factor; UC, ulcerative colitis; WT, wild-type.**

0016-5085/$36.00
http://dx.doi.org/10.1053/j.gastro.2014.04.007

primarily by NF-κB complexes containing the RelA subunit (also known as p65) or its paralog c-Rel. Under basal conditions, these complexes are kept in the cytosol through interactions with the inhibitory IκB proteins. Their activation requires IκB degradation, an event triggered by a critical kinase complex known as IκB kinase that sits at the cross-roads of numerous signaling pathways. After signaling inputs abate, homeostatic mechanisms that restore basal NF-κB activity are essential for the physiologic function of this pathway. The induction of IκB gene expression,[5] or the expression of IκB kinase inhibitory proteins, such as A20 or CYLD,[6,7] participate in the timely termination of NF-κB activity. The expression of these factors is under the control of NF-κB itself, thus providing negative feedback loops in the pathway. In addition, it has been recognized that ubiquitination and proteasomal degradation of RelA is critical to terminate transcription of a variety of genes.[8–13] One ligase responsible for these effects contains the scaffold protein Cul2 in association with copper metabolism MURR1 domain containing 1 (COMMD1),[10,12] a prototypical member of the COMMD protein family.[14]

In addition to its role in NF-κB regulation,[12,15] COMMD1 has been implicated in a variety of cellular processes, including copper transport,[16] electrolyte balance,[17–19] and hypoxia responses.[20] Given these pleiotropic functions, it has remained unclear whether this factor plays a physiologically important role in the control of inflammation in vivo and whether it could play a role in chronic inflammatory diseases. Here, we report that myeloid-specific deficiency of *Commd1* leads to more intense activation of lipopolysaccharide (LPS)-inducible genes and is associated with more severe inflammation. In addition, we present genetic evidence linking gene variants associated with reduced *COMMD1* expression to risk for UC in human beings, highlighting the physiologic importance of this gene in immunity and IBD pathogenesis.

Materials and Methods

Human Studies

All procedures involving human subjects were reviewed and approved by the respective institutional review boards (at the University of Texas Southwestern Medical Center, the Mayo Clinic, and the Tel-Aviv Sourasky Medical Center). Circulating leukocytes and intestinal biopsy specimens were obtained at the time of endoscopy as part of the patients' ongoing medical care.

Genome-Wide Association Studies and Quantitative Trait Locus Analysis

Genetic association data were obtained from the 1000 genomes imputed meta-analysis from 15 genome-wide association studies of CD and/or UC conducted by the International IBD Genetic Consortium (IIBDGC).[3] We conducted *cis*-expression quantitative trait locus (cis-eQTL) mapping on whole peripheral blood of 2 cohorts: 1240 samples from a previously published study[21] and 891 samples from the Estonian Biobank, both hybridized to Illumina (San Diego, CA) HT12-v3 oligonucleotide arrays using methodology as described in detail elsewhere.[22]

Statistical Analysis

In all graphs, the mean is presented and the error bars correspond to the SEM. Statistical comparisons between mean values were performed using a 1-tailed, heteroscedastic, Student *t* test. For nonparametric variables, the chi-square test was used. Survival curves were examined using the Kaplan–Meier analysis.

All other materials and methods are described in the Supplementary Materials and Methods section.

Results

Commd1 Represses Proinflammatory Gene Expression in Myeloid Cells

To evaluate the potential role of COMMD1 in inflammation, and given the known embryonic lethality that results from complete *Commd1* deficiency in mice,[23] we generated a tissue-specific mouse model of *Commd1* deficiency.[24] First, *Commd1* was selectively deleted in myeloid cells (Mye-knockout [K/O]), a critical lineage in innate immunity, leading to the expected loss of Commd1 expression in macrophages (Supplementary Figure 1*A*). Mye-K/O mice were healthy and B-lymphocyte ($B220^+$) and T-lymphocyte populations ($CD3^+$ and CD4/CD8) were not significantly different in the spleen or mesenteric lymph nodes (Supplementary Figure 1*B* and *C*). Similarly, myeloid populations, including granulocytes ($Ly6G^+$), monocytes and macrophages ($CD11b^+$, $Ly6C^+$, and F4/80), and dendritic cells ($CD11c^{high}$ and $CD11c^{intermediate}$) were not significantly different in Mye-K/O mice (Supplementary Figure 1*B–D*). In line with previous observations,[12,25,26] *Commd1* deficiency did not alter substantially the phosphorylation or turnover of IκB (Figure 1*A*), but had a profound effect on RelA ubiquitination (Figure 1*B*).

Next, using bone marrow–derived myeloid cells (BMDMs) from the Mye-K/O mice, we assessed the impact of *Commd1* on the LPS transcriptional response at a genome-wide level. High-density microarray experiments indicated that 1008 genes were regulated by LPS at least 3-fold in 2 independent series of experiments (Figure 1*C*, and Supplementary Tables 1–3). In addition, the expression of 225 genes was found to be regulated by *Commd1* (Supplementary Tables 1 and 2). Notably, the vast majority of *Commd1*-regulated genes (219 of 225) also was regulated by LPS, and only few *Commd1* target genes (6 of 225) were outside the LPS transcriptional response (Supplementary Tables 2 and 3). Hierarchical clustering of these 225 genes was used to visualize the pattern of deregulated expression in *Commd1*-deficient myeloid cells. Both early and late LPS-inducible genes were affected by *Commd1* deficiency (Figure 1*D*). In most instances, the changes observed consisted of increased gene expression, which often were noted even at basal levels (Figure 1*E*).

To further understand the effect of *Commd1* on gene expression in myeloid cells, we performed a functional

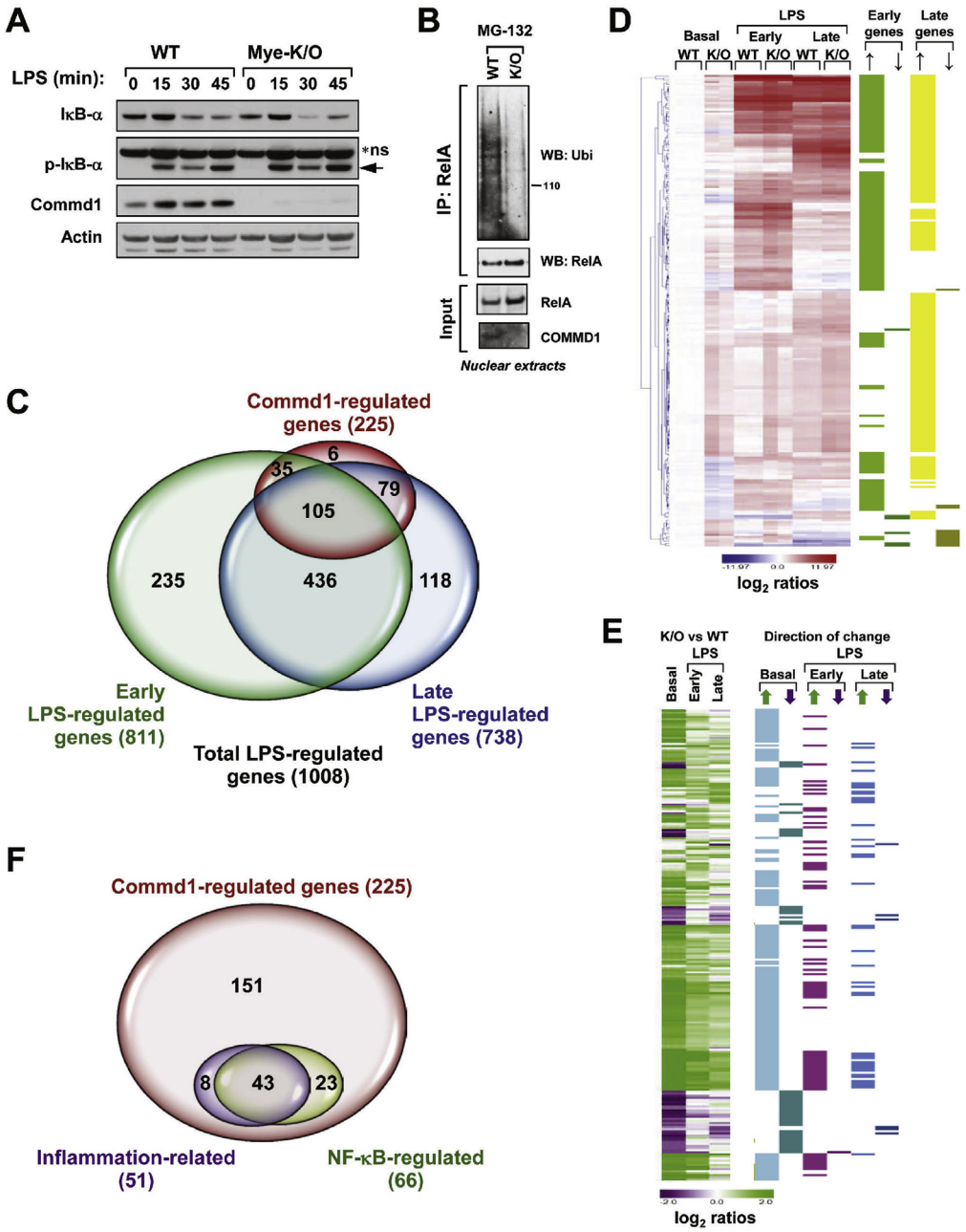

Figure 1. *Commd1* regulates the LPS transcriptional program in myeloid cells. (*A*) Commd1 does not affect IκB turnover in BMDMs. IκB-α phosphorylation (p-IκB-α) and degradation after LPS treatment were examined by Western blotting. *ns, nonspecific band (*arrow* points to p-IκB-α). (*B*) *Commd1* deficiency reduces RelA ubiquitination. *Commd1*-deficient mouse embryo fibroblasts (K/O) or control cells (WT) were used to detect ubiquitinated RelA by ubiquitin immunoblotting of immunoprecipitated RelA. (*C*) Gene expression differences resulting from *Commd1* deficiency substantially overlap with the LPS response. BMDMs from WT and Mye-K/O mice were used in duplicate microarray analysis to ascertain genes regulated by *Commd1* or by LPS (100 ng/mL) at early (3 h) or late (24 h) time points. The degree of overlapping genes is presented in Venn diagram form. (*D*) Hierarchical cluster analysis of *Commd1*-regulated genes during the LPS response. Expression levels normalized to basal expression in WT samples is shown as color-coded $\log_2$-transformed ratios. The gene induction pattern, either early (>3-fold induction at 3 h) or late LPS response (>3-fold induction at 24 h), also is indicated. The specific effect of *Commd1* deficiency is noted by *up arrows* or *down arrows*. (*E*) The genes analyzed in *panel D* are reanalyzed by calculating ratios between K/O and WT BMDMs, displayed in a color-coded $\log_2$-transformed manner. The direction of change is indicated in adjacent columns by *up arrows* or *down arrows*. (*F*) Venn diagram of *Commd1*-regulated genes, indicating those involved in inflammatory responses or regulated by NF-κB.

analysis using the Kyoto encyclopedia of genes and genomes (KEGG) database. This showed that only 51 genes (23%) participate in immune regulation (as defined by any of a number of KEGG entries) (Supplementary Table 4), indicating that a large number of *Commd1* gene targets in myeloid cells are not known inflammatory regulators

(Figure 1*F*). Next, we assessed the contribution of NF-κB regulation to the effects noted in *Commd1*-deficient myeloid cells. To that end, NF-κB regulation of genes of interest was ascertained through 2 overlapping approaches: first, using a curated database of published NF-κB gene targets (publicly available at www.NF-κB.org), and second, using chromatin immunoprecipitation (ChIP) for RelA followed by sequencing (ChIP-seq) in LPS-stimulated BMDMs.[27] This indicated that only 66 genes regulated by *Commd1* (29%) (Supplementary Table 4) are known NF-κB or RelA targets, suggesting that a substantial proportion of the effects of Commd1 are either secondary or mediated through other transcriptional regulators.

Commd1 Exerts Gene-Selective Effects Among NF-κB–Regulated Targets

Altogether, these findings suggest a substantial repressive role for *Commd1* on the LPS response in myeloid cells and confirmed a negative regulatory role for *Commd1* on selected NF-κB–regulated genes. Indeed, quantitative reverse-transcription polymerase chain reaction analysis corroborated that certain NF-κB target genes were selectively regulated (eg, *Mx1*, *Cd86*, and *Sell*) (Figure 2*A*), whereas others were relatively insensitive to *Commd1* deficiency (such as *Il6*, *Tnfaip3*, and *Mmp13*) (Supplementary Figure 2*A*). These findings are in line with previous reports of gene-specific effects for COMMD1 in cancer cell lines.[12] Enhanced expression of selected genes that are not regulated directly by NF-κB was confirmed as well (Figure 2*B*). Interestingly, in contrast to these effects, several hypoxia-induced genes were not affected by *Commd1* deficiency in BMDMs (Supplementary Figure 2*B*), despite its reported role in hypoxia-dependent gene expression.[20,23] In aggregate, the data indicate that *Commd1* primarily exerts a gene-selective repressive function on the LPS response.

Myeloid Deficiency of Commd1 Leads to Exaggerated Inflammatory Responses In Vivo

In view of the effects of *Commd1* on LPS-induced gene expression, we used 2 models to contrast the inflammatory response of Mye-K/O mice and wild-type (WT) littermate controls. First, we used the cecal ligation and puncture model of polymicrobial sepsis. Animal survival was compromised in Mye-K/O mice compared with WT controls (Figure 3*A*). In contrast, cultures of peritoneal fluid showed lower bacterial counts in the Mye-K/O mice (Figure 3*B*), indicating that their increased mortality was not caused by greater bacterial load. Rather, after accounting for bacterial invasion (by examining animals with negative bacterial cultures), we found that Mye-K/O mice had increased cytokine expression (Figure 3*C*), suggesting that exaggerated proinflammatory gene expression was responsible for their increased susceptibility to sepsis. Next, animals were challenged directly with intraperitoneal LPS injection. Once more, Mye-K/O mice showed greater mortality (Figure 3*D*) and increased morbidity (Supplementary Figure 3*A*). Tissue injury, manifested by lactate dehydrogenase release in plasma, also was more pronounced in Mye-K/O mice (Supplementary Figure 3*B*), which also displayed greater plasma increases of interleukin (Il)6 and tumor necrosis factor (Tnf) (Figure 3*E*). In contrast, plasma levels of the anti-inflammatory cytokine Il10 were comparable with WT. Tissue expression of proinflammatory genes was more pronounced in Mye-K/O mice, as exemplified by *Tnf*, as well as other proinflammatory genes (Figure 3*F* and Supplementary Figure 4). Altogether, these data indicate that *Commd1* deficiency in the myeloid lineage leads to more profound acute inflammatory responses.

Reduced Expression of COMMD1 Is a Common Feature of IBD

Given the findings made in the Mye-K/O mouse model, we decided to explore whether *COMMD1* could play a role in the pathophysiology of inflammatory disorders in human beings, choosing IBD as a disease model. To this end, we evaluated the expression of *COMMD1* in IBD patients. We found that *COMMD1* messenger RNA (mRNA) levels in colonic endoscopic biopsy specimens were reduced in an Israeli cohort of patients with colitis (n = 29, 18 with Crohn's disease and 11 with ulcerative colitis) compared with unaffected controls (n = 16; $P = .04$) (Figure 4*A*, *left*). This finding was replicated in an independent patient cohort in the United States ($P = .04$, 22 normal controls and 17 patients with IBD, 9 of whom had CD and 8 had UC) (Supplementary Figure 5). Similarly, we found that *COMMD1* mRNA was reduced in circulating leukocytes from IBD patients with active disease (n = 12, 9 with CD and 3 with UC) compared with normal individuals (n = 14; $P = .001$) (Figure 4*A*, *right*). Moreover, in a murine model of colitis induced by dextran sodium sulfate (DSS) administration, we also observed decreased mRNA and protein expression of *Commd1* and other *Commd* genes in the colon (Figure 4*B* and *C*). In aggregate, the data indicate that mucosal inflammation is associated with decreased *COMMD1* gene expression in clinical and experimental situations.

Genetic Variants Associated With Decreased COMMD1 Expression Are Associated With UC Risk

In view of the reduced expression of *COMMD1* in IBD patients, we investigated whether genetic polymorphisms of this gene might affect IBD risk in human beings. Interestingly, genome-wide association studies have linked an intergenic region near *COMMD1* to the risk for various inflammatory conditions including IBD (Figure 4*D*),[3,28–32] but the precise gene responsible for these effects remains unknown.

We began by interrogating the most recent meta-analysis of genome-wide association studies for CD and UC[3] by the IIBDGC, which currently is available on the Ricopili server (www.broadinstitute.org/mpg/ricopili/). These data indicated a suggestive association signal with UC for single-nucleotide polymorphisms (SNPs) located

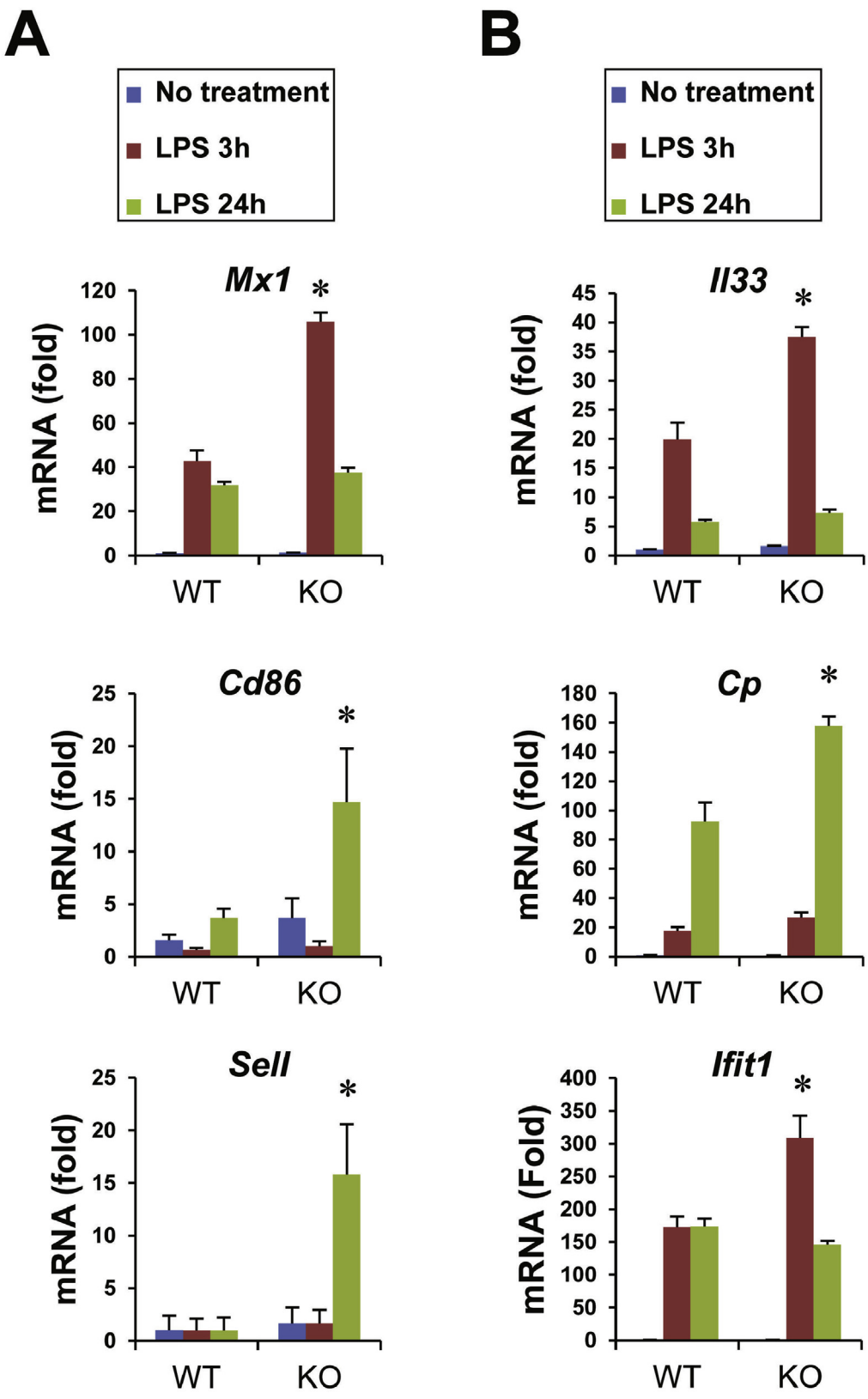

Figure 2. Gene-selective effects of *Commd1* on NF-κB–regulated targets. BMDMs (2 mice per group, with triplicate cultures per mouse) were stimulated with LPS, and gene expression was determined by quantitative reverse-transcription polymerase chain reaction. (*A*) Selected NF-κB target genes are shown, and other (*B*) LPS-inducible genes that are not NF-κB targets also are shown.

just downstream of *COMMD1*, including rs3943540 ($P = 7.89 \times 10^{-5}$) and rs921319 ($P = 7.47 \times 10^{-5}$) (Figure 4*E*). Interestingly, both SNPs are in linkage disequilibrium with each other ($r^2 = 1$, $D' = 1$). Additional analysis of the 1000 genomes–imputed IIBDGC UC and CD meta-analyses also showed a suggestive association with

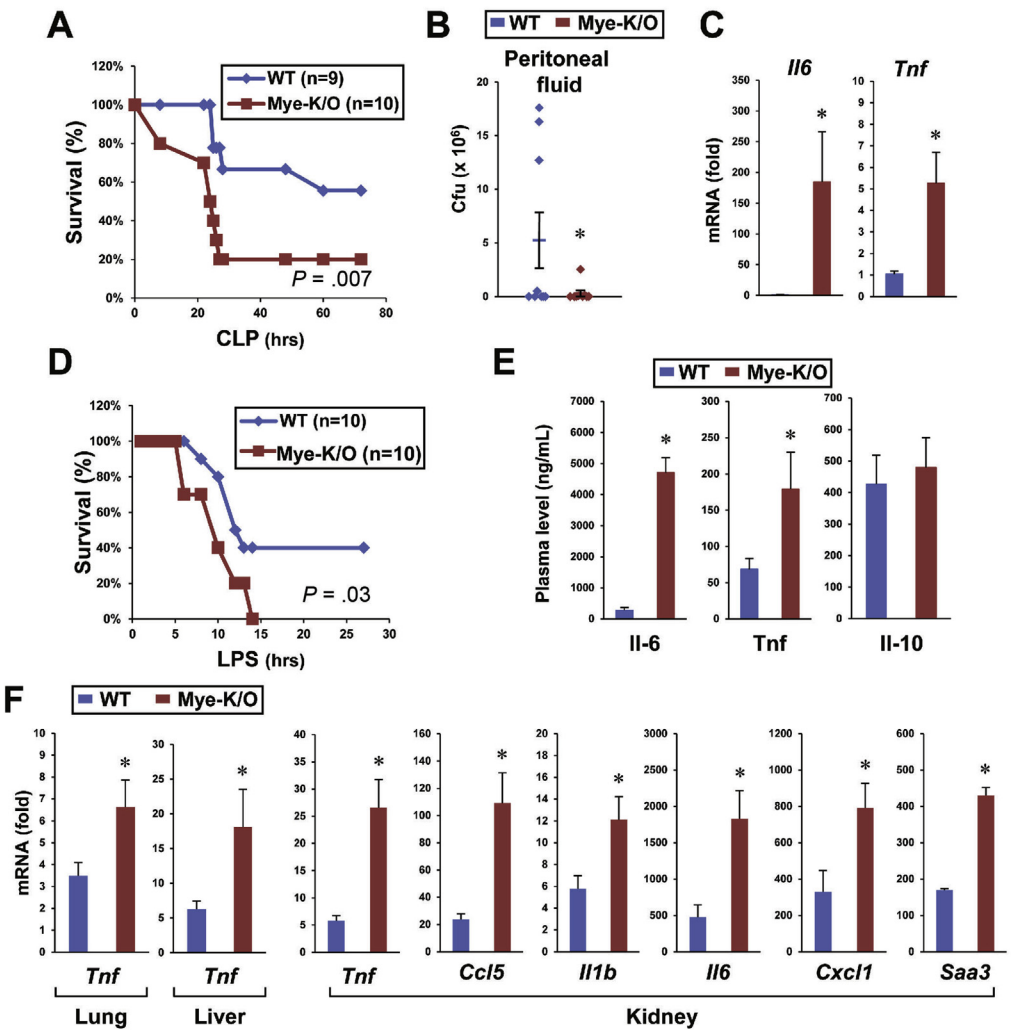

Figure 3. Mye-K/O mice have a more severe sepsis response. (*A*) Cecal ligation and puncture leads to a higher mortality rate in Mye-K/O mice. Mye-K/O animals (*Commd1*$^{F/F}$, LysM-Cre) were compared with WT littermate controls (*Commd1*$^{F/F}$). Survival without the need for euthanasia was plotted and the Kaplan–Meier estimate was calculated. (*B*) Peritoneal cultures yield lower bacterial counts in Mye-K/O mice (9 mice in each group). Colony forming units (Cfu) in blood agar were determined by progressive dilution. (*C*) Induction of proinflammatory gene expression is greater in Mye-K/O mice. Tissue RNA was analyzed by quantitative reverse-transcription polymerase chain reaction (in kidney). To normalize for bacterial load, animals with no detectable bacterial counts were used for this analysis (WT, 4 mice; Mye-K/O, 6 mice). (*D*) Mye-K/O mice have greater mortality after LPS administration. Survival was analyzed as in *panel A*. (*E*) Plasma levels of Il6, Tnf, and Il10 were determined in Mye-K/O mice (n = 9) and WT controls (n = 10) at the time of euthanasia in the LPS model. (*F*) LPS induction of proinflammatory genes was determined by quantitative reverse-transcription polymerase chain reaction in tissues of Mye-K/O mice (n = 10) and WT controls (n = 10). *$P < .05$.

UC for a SNP located in the same region, rs6545924 ($P = 2.27 \times 10^{-5}$; odds ratio, 1.104; 95% confidence interval of the odds ratio, 1.06–1.15).

Epigenetic analysis in myeloid cells performed by the Encyclopedia of DNA Elements (ENCODE) project[33] showed that this genomic locus displays features of a gene regulatory region (Figure 4*D* and *E*), such as histone 3 lysine 4 monomethylation and lysine 27 acetylation, both associated with active enhancers.[34] In agreement with this notion, the SNP and CNV Annotation (SCAN) database[35] indicates that there is a significant eQTL effect of rs921319 on *COMMD1* gene expression. To further examine the possibility that these variants have an effect on *COMMD1* expression, we conducted *cis*-eQTL mapping on whole peripheral blood of 2 cohorts (1240 samples previously studied[21] and 891 samples from the Estonian Biobank). Because the SNPs in question were not present in our eQTL data set, we tested rs921320, located in very close proximity to rs921319 and a perfect proxy SNP for rs6545924 ($r^2 = 0.9$, D' = 1). We observed a significant eQTL effect of rs921320 on *COMMD1* expression, with the same allelic direction for the Dutch and Estonian cohorts (the *P* values for individual cohorts were .057 and .0099, respectively; with a weighted Z-method meta-analysis $P = .0033$). The A–allele of rs921320, which is linked to the risk allele for rs6545924, was associated with reduced expression of *COMMD1* (Figure 4*F*). On the other hand, we did not observe any eQTL effects of rs921320 on the 2

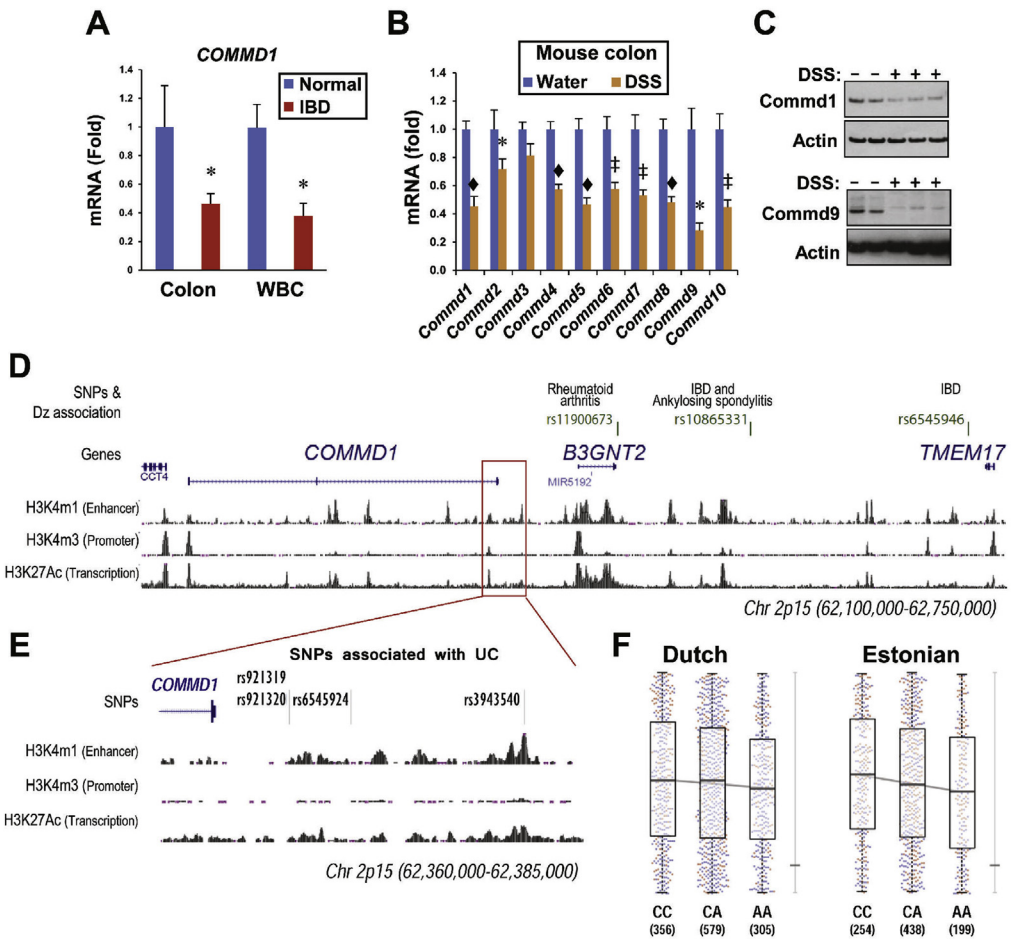

Figure 4. Lower *COMMD1* expression is linked to IBD. (*A*) *COMMD1* gene expression is suppressed in IBD patients. *COMMD1* mRNA expression was determined by quantitative reverse transcription polymerase chain reaction in endoscopic colonic biopsy specimens from IBD patients with colitis (n = 29, 18 with CD and 11 with UC) and normal controls (n = 17). Similarly, *COMMD1* mRNA levels in white blood cells (WBCs) were determined in IBD patients (n = 12, 9 with CD and 3 with UC) and unaffected controls (n = 14). (*B* and *C*) *Commd* gene expression at the (*B*) mRNA level was decreased similarly in colonic tissue after DSS-induced acute colitis (7 mice in the DSS group compared with 8 mice in the water group), and (*C*) this was shown at the protein level for Commd1 and Commd9. $^{*}P < .05$, $^{‡}P < .001$, $◆P < .0001$. (*D*) Polymorphisms near *COMMD1* are associated with UC risk. A map of the 2p15 locus, including SNPs previously implicated in inflammatory diseases, is shown. The region located 3' of the *COMMD1* gene, where SNPs associated to UC were found, is marked by a *red box*. (*E*) A closer view of the location of the SNPs of interest downstream of *COMMD1* is shown, including chromatin modifications such as histone 3 K4 monomethylation (H3K4m1), trimethylation (H3K4m3), and histone 3 K27 acetylation (H3K27Ac). (*F*) *cis*-eQTL analysis for rs921320 in 2 independent cohorts. *COMMD1* gene expression (in the y axis) is shown in a box plot for all 3 genotypes for this SNP (CC, CA, or AA). The *horizontal bar* in the box is the median, the *top* and *bottom* of the box show the interquartile range (Q3 - Q1); the whiskers show the quartile + 1.5× the interquartile range. The number of individuals in each group is indicated (under the genotype); men and women are denoted by *blue dots* and *red dots*, respectively.

other neighboring genes, *B3GNT2* or *TMEM17*. Altogether, these findings suggest that genetic variation in the 3' region of *COMMD1*, which has regulatory effects on gene expression, is linked to risk for UC.

Myeloid Cell Deficiency of Commd1 Leads to More Severe Colitis

To further examine the possible involvement of *COMMD1* in IBD pathogenesis, we began by assessing the in situ expression of this gene in the colon. Immunofluorescence staining of mouse colon tissue showed staining in the epithelium as well as in mononuclear cells in the lamina propria (Supplementary Figure 6). Furthermore, confocal microscopy images confirmed that resident lamina propria macrophages ($F4/80^{+}$) are also COMMD1 positive, in agreement with Western blot analysis of primary myeloid cells (Figure 1*A*). With this in mind and in view of the known contributions of both epithelial and myeloid cells in the pathogenesis of human and murine colitis,[36,37] we evaluated the role of this gene in this disease process using both epithelial and myeloid cell–specific knockout mice.

First, we used the DSS model, which triggers colonocyte injury and an innate immune response to luminal bacteria that results in acute colitis. Mye-K/O mice showed more

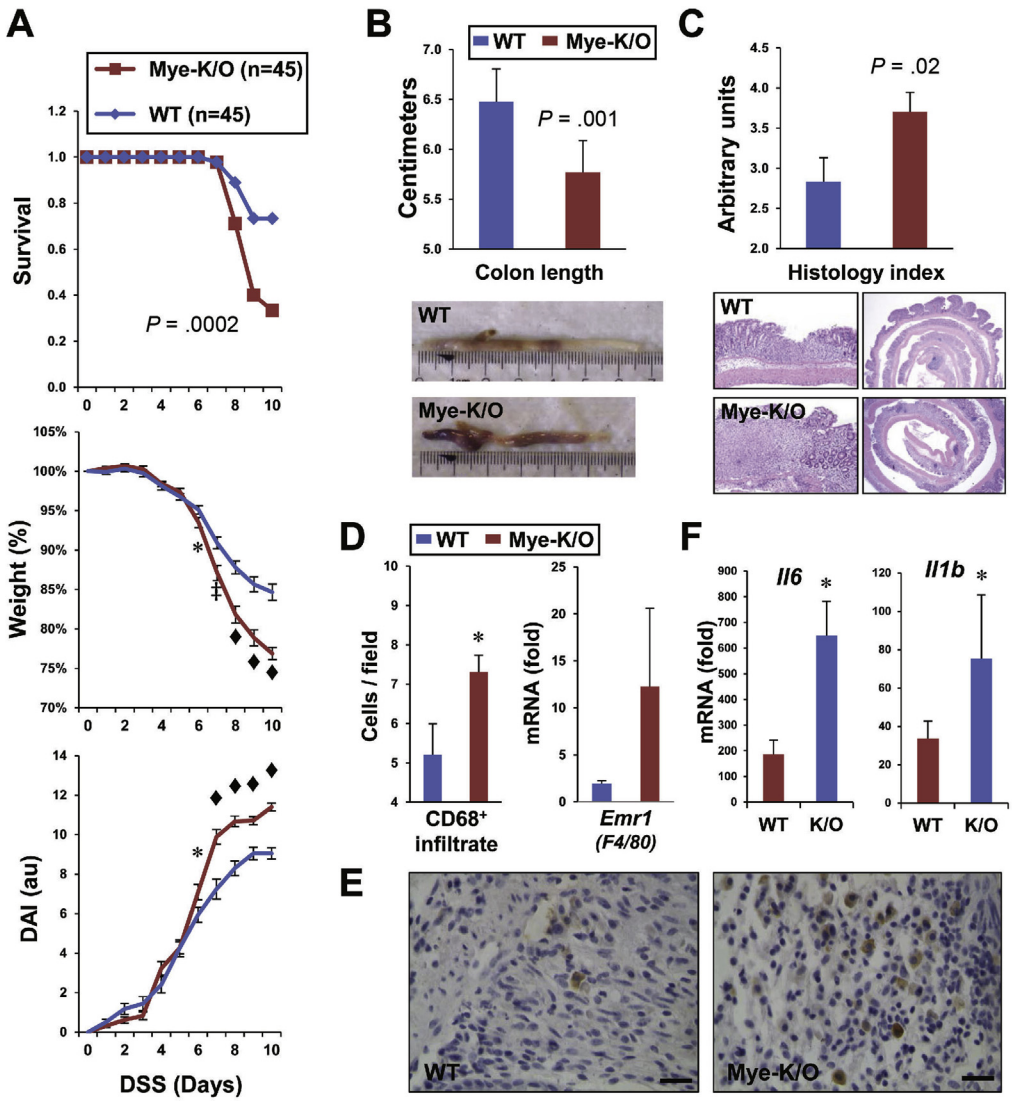

Figure 5. Myeloid deficiency of *Commd1* predisposes to more severe colitis. (*A*) Worse survival, weight loss, and disease activity index (DAI) were noted in Mye-K/O mice compared with wild-type littermate controls during acute DSS-induced colitis. *$P < .05$, ‡$P < .001$, ◆$P < .0001$. (*B*) Colon length was significantly shorter in Mye-K/O mice (n = 26) after acute colitis compared with WT controls (n = 20). Representative images are shown. (*C*) Worse tissue injury also was evident histologically. By using a severity score, colonic sections were examined (11 Mye-K/O and 9 WT mice). Representative histologic sections are shown. (*D* and *E*) Expansion of macrophage populations in the colonic mucosa of Mye-K/O mice. In the *left panel*, the number of $CD68^+$ cells present in the mucosa was assessed by immunohistochemistry in a tissue microarray of DSS colitis samples (Mye-K/O, 13 samples; WT, 12 samples). In the *right panel*, the colonic expression of the macrophage marker gene *Emr1* (*F4/80*) was determined by quantitative reverse-transcription polymerase chain reaction (Mye-K/O, 18 samples; WT, 23 samples). (*E*) Representative images of the CD68 immunohistochemistry are shown. *Scale bar*: 20 μm. (*F*) RNA extracted from colonic tissue was used for quantitative reverse-transcription polymerase chain reaction analysis for the genes indicated (Mye-K/O, 18 samples; WT, 23 samples). au: arbitrary units.

severe disease than WT animals, with excess mortality, more profound weight loss, and worse disease activity (Figure 5*A*). In agreement with this, colon shortening (a macroscopic marker of tissue injury) and histologic evaluation of the colonic mucosa both indicated more damage in Mye-K/O mice (Figure 5*B* and *C*). In contrast to these results, *Commd1* inactivation in the intestinal epithelium did not result in any appreciable alteration of DSS-induced colitis (Supplementary Figure 7). The more severe inflammatory response in Mye-K/O mice correlated with greater numbers of $CD68^+$ myeloid cells in the colon as seen by immunohistochemistry (Figure 5*D*, *left panel*, and *E*), and a consistent trend was observed at the mRNA level for the macrophage-specific gene *Emr1* (*F4/80*, Figure 5*D*, *right panel*). In addition, Mye-K/O mice showed increased expression of proinflammatory genes, such as *Il6* and *Il1b* (Figure 5*F*). However, myeloid and lymphoid populations in the mesenteric lymph node (Supplementary Figure 8) and the spleen (not shown), were not significantly different between the groups.

Myeloid Cell Deficiency of Commd1 Promotes Colitis–Dysplasia Progression

Further analysis indicated that recurrent DSS administration, which mimics the chronic nature of IBD, also resulted in more severe disease in Mye-K/O mice, manifested as greater weight loss (Figure 6*A*) and more severe anemia (Figure 6*B*). Colonic tissue from these animals also produced greater amounts of several proinflammatory factors such as Tnf (Figure 6*C* and Supplementary Figure 9). In addition, azoxymethane followed by recurrent DSS treatments was used to examine progression to dysplasia. In this model, Mye-K/O mice also showed more severe disease, as evidenced by more severe colonic shortening, splenomegaly, and histologic distortion of the mucosal architecture (Figure 6*D*). Moreover, after 7 weeks of treatment, Mye-K/O mice had a greater propensity to develop dysplasia, high-grade dysplasia, or multifocal dysplasia as assessed histologically (Figure 6*D*). By 10 weeks, small adenomas could be visualized, but the total number of lesions was not increased in Mye-K/O mice (Figure 6*E*). Nevertheless, only Mye-K/O mice developed proximal colonic tumors and there was a tendency for the tumor burden to be greater in these animals as a result of greater adenoma volume (Figure 6*E*). In colonic tissue, Mye-K/O animals showed greater NF-κB activation as evidenced by the ratio of the transcriptionally active form of RelA (phosphorylated at Ser536) to total RelA. However, STAT3 activation, another pathway known to promote cancer in the context of chronic tissue

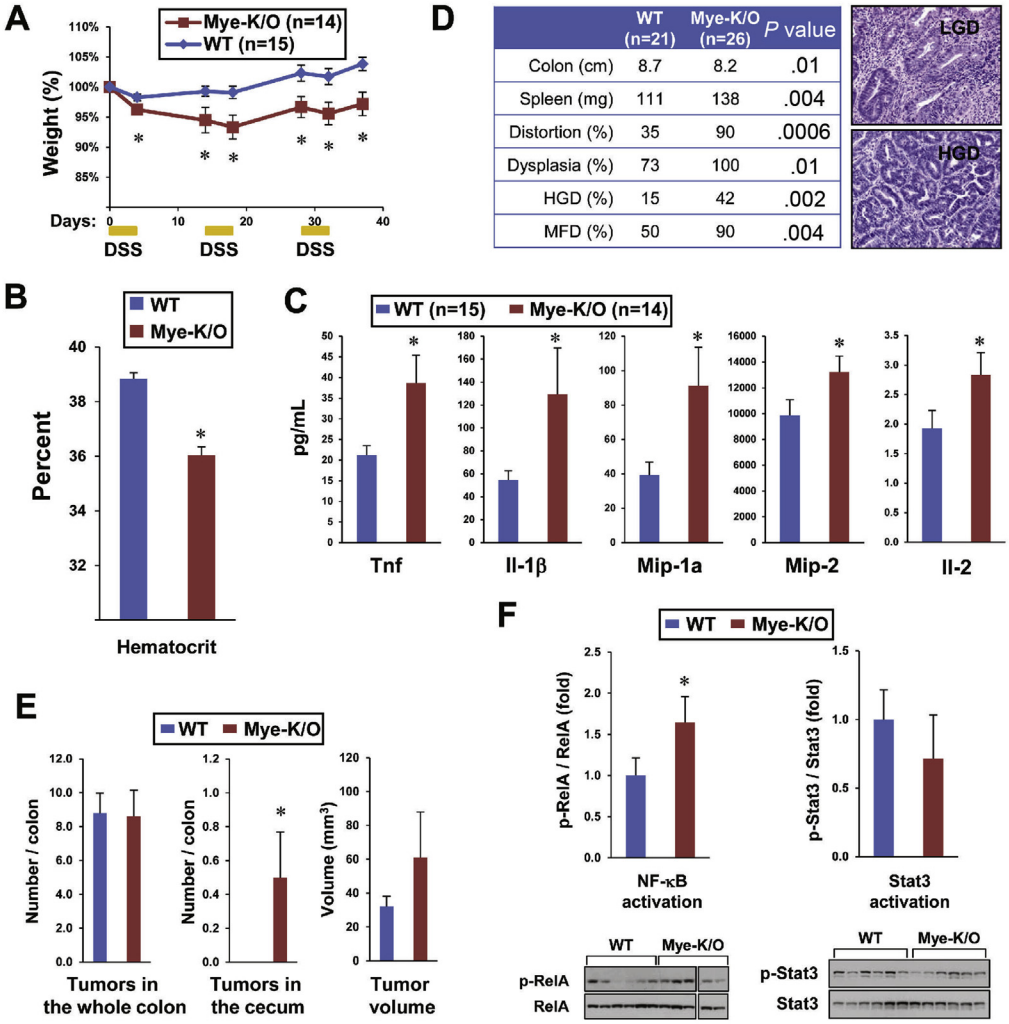

Figure 6. *Commd1* deficiency leads to worse chronic colitis and transition to dysplasia. (*A*) Recurrent administration of DSS caused more weight loss in Mye-K/O mice. (*B*) Chronic colitis led to more severe anemia in Mye-K/O mice (5 mice per group). (*C*) Proinflammatory cytokine production is increased in colonic tissue of Mye-K/O mice. Colonic full-thickness tissue harvested from colitic mice was cultured overnight and the secretion of cytokines into the growth media was determined. (*D*) Progression to dysplasia was worse in Mye-K/O animals. Azoxymethane was administered before chronic colitis induction and dysplasia was assessed histologically at 7 weeks. Representative images are displayed. (*E*) Tumor number and volume in mice at 10 weeks of colitis/dysplasia induction is shown. *$P < .05$. (*F*) Greater NF-κB activation in inflamed colonic tissue of Mye-K/O mice. Activation of NF-κB/RelA and Stat3 was assessed in inflamed colonic tissue of animals treated with AOM/DSS. Western blot analysis was performed with tissue lysates and the active phosphorylated form was quantitated and normalized to expression of the respective target. HGD, high-grade dysplasia; LGD, low-grade dysplasia; MFD, multifocal dysplasia.

inflammation,[38] was not altered in these mice (Figure 6*F*). Altogether, these data highlight a role for myeloid cell expression of Commd1 in chronic colonic inflammation and progression to dysplasia.

Discussion

COMMD1 plays an essential role to restrain the activity of NF-κB, a master regulator of inflammation. Specifically, COMMD1 acts to terminate NF-κB transcriptional activation through the ubiquitin-mediated degradation of NF-κB subunits. A detailed molecular mechanism by which COMMD1 restrains NF-κB has been examined and reported previously.[8,10,12,13] The studies presented here confirm the negative regulatory role of this factor on the NF-κB pathway,[10,12,13,15] and also underscores the gene-selective nature of these effects. Moreover, the studies in this model corroborate that key aspects of the reported mechanism are evident in the knockout mice, namely normal IκB phosphorylation and turnover, but diminished ability to terminate NF-κB transcriptional activity (ie, reduced RelA/p65 ubiquitination). Importantly, this study investigates the physiological relevance of these events in disease pathogenesis. The data indicate that COMMD1 expression in the myeloid compartment plays an important role in the regulation of inflammatory responses in vivo. Given that diverse functions have been reported for this gene,[17,39–41] this report fills a critical void by underscoring that COMMD1 participates in immune regulation. In addition, the results also suggest that COMMD1 has broader effects on proinflammatory gene expression programs that might extend beyond the NF-κB pathway. Whether these effects are the result of secondary perturbations or are the result of direct regulation of transcription factor(s) other than NF-κB, should be examined further in the future.

In the context of intestinal inflammation and progression to cancer, previous studies have underscored the importance of epithelial and myeloid cells in these processes.[14,37,38] In particular, epithelial intrinsic NF-κB activation has been shown to be a protective response that promotes cell survival and barrier function,[42] and myeloid cell NF-κB activation is important in sustaining the inflammatory response.[36] The increased propensity to inflammation and colitis observed as a result of myeloid cell deficiency of *Commd1* is in agreement with this paradigm and suggests that the immune regulatory roles of this gene are physiological. In addition, the increased progression to dysplasia in Mye-K/O mice is in agreement with the role of myeloid cells in promoting tumor growth through various proinflammatory cytokines.[43] In this regard, our model displays increased production of Tnf and greater tissue activation of NF-κB, both of which have been shown to promote cancer progression in the setting of colitis.[36,44] In addition, we also found no appreciable phenotype of enterocyte-specific deficiency of *Commd1*, which stands in contrast to other models of disrupted NF-κB activity in the epithelium.[36,42] This may reflect the fact that unlike other models, cell survival genes are not regulated by COMMD1 in the transcriptome analysis presented here. Furthermore, it suggests that other reported roles of *Commd1*, such as the regulation of various transport mechanisms, may be more relevant in these cells.

These observations in the animal model, coupled with the finding that genetic variants linked to lower *COMMD1* expression also are associated with an increased risk for UC, suggest that this gene participates in the pathogenesis of this disorder in human beings. In this context, it is important to note a recent report of a risk association for *COMMD7*, another member of the *COMMD* gene family.[45] Moreover, COMMD1 acts in concert with Cul2 to promote RelA ubiquitination,[10,12,13] and the *CUL2* gene has been linked to IBD susceptibility.[46] Additional studies, including ongoing resequencing efforts, will be required to validate the genetic association seen here with greater statistical confidence. However, the aggregate of our data and published reports suggest the possibility that homeostatic mechanisms that restore NF-κB to its basal state, when decreased, may enhance the risk for IBD.

Our studies also identified that inflammation can lead to suppressed expression of *COMMD1*, as seen in patients with colitis as well as in animal models. Our data suggest that this is likely the consequence rather than the cause of inflammation in human disease because this suppression can be induced by inflammation itself in animal studies. The decrease in *COMMD1* expression probably plays a physiologic role in the initiation of an appropriate inflammatory response, but in view of the more severe inflammatory responses seen when this gene is deleted in myeloid cells, persistent *COMMD1* suppression probably is maladaptive during chronic inflammation. Therefore, this work highlights the need to gain a refined understanding of the molecular events that control *COMMD1* gene expression in the setting of inflammation. With this knowledge, we may begin to envision potential interventions that might restore gene expression, which could be tested for their therapeutic potential in chronic inflammatory disorders.

Supplementary Material

Note: To access the supplementary material accompanying this article, visit the online version of *Gastroenterology* at www.gastrojournal.org, and at http://dx.doi.org/10.1053/j.gastro.2014.04.007.

References

1. Kaser A, Zeissig S, Blumberg RS. Inflammatory bowel disease. Annu Rev Immunol 2010;28:573–621.
2. Hayden MS, Ghosh S. NF-κB, the first quarter-century: remarkable progress and outstanding questions. Genes Dev 2012;26:203–234.
3. **Jostins L, Ripke S**, Weersma RK, et al. Host-microbe interactions have shaped the genetic architecture of inflammatory bowel disease. Nature 2012;491:119–124.
4. Lees CW, Barrett JC, Parkes M, et al. New IBD genetics: common pathways with other diseases. Gut 2011;60:1739–1753.

5. **Hoffmann A, Levchenko A**, Scott ML, et al. The IκB-NF-κB signaling module: temporal control and selective gene activation. Science 2002;298:1241–1245.
6. Kovalenko A, Chable-Bessia C, Cantarella G, et al. The tumour suppressor CYLD negatively regulates NF-κB signalling by deubiquitination. Nature 2003;424:801–805.
7. Wertz IE, O'Rourke KM, Zhou H, et al. De-ubiquitination and ubiquitin ligase domains of A20 downregulate NF-κB signalling. Nature 2004;430:694–699.
8. Natoli G, Chiocca S. Nuclear ubiquitin ligases, NF-κB degradation, and the control of inflammation. Sci Signal 2008;1:pe1.
9. Saccani S, Marazzi I, Beg AA, et al. Degradation of promoter-bound p65/RelA is essential for the prompt termination of the nuclear factor κB response. J Exp Med 2004;200:107–113.
10. Mao X, Gluck N, Li D, et al. GCN5 is a required cofactor for a ubiquitin ligase that targets NF-κB/RelA. Genes Dev 2009;23:849–861.
11. Ryo A, Suizu F, Yoshida Y, et al. Regulation of NF-κB signaling by Pin1-dependent prolyl isomerization and ubiquitin-mediated proteolysis of p65/RelA. Mol Cell 2003;12:1413–1426.
12. Maine GN, Mao X, Komarck CM, et al. COMMD1 promotes the ubiquitination of NF-κB subunits through a Cullin-containing ubiquitin ligase. EMBO J 2007;26:436–447.
13. Geng H, Wittwer T, Dittrich-Breiholz O, et al. Phosphorylation of NF-κB p65 at Ser468 controls its COMMD1-dependent ubiquitination and target gene-specific proteasomal elimination. EMBO Rep 2009;10:381–386.
14. Burstein E, Hoberg JE, Wilkinson AS, et al. COMMD proteins: a novel family of structural and functional homologs of MURR1. J Biol Chem 2005;280:22222–22232.
15. Ganesh L, Burstein E, Guha-Niyogi A, et al. The gene product Murr1 restricts HIV-1 replication in resting $CD4^+$ lymphocytes. Nature 2003;426:853–857.
16. van de Sluis B, Rothuizen J, Pearson PL, et al. Identification of a new copper metabolism gene by positional cloning in a purebred dog population. Hum Mol Genet 2002;11:165–173.
17. Biasio W, Chang T, McIntosh CJ, et al. Identification of Murr1 as a regulator of the human δ epithelial sodium channel. J Biol Chem 2004;279:5429–5434.
18. Drevillon L, Tanguy G, Hinzpeter A, et al. COMMD1-mediated ubiquitination regulates CFTR trafficking. PLoS One 2011;6:e18334.
19. Smith L, Litman P, Liedtke CM. COMMD1 interacts with the COOH terminus of NKCC1 in Calu-3 airway epithelial cells to modulate NKCC1 ubiquitination. Am J Physiol Cell Physiol 2013;305:C133–C146.
20. **van de Sluis B, Mao X**, Zhai Y, et al. COMMD1 disrupts HIF-1α/β dimerization and inhibits human tumor cell invasion. J Clin Invest 2010;120:2119–2130.
21. Fu J, Wolfs MG, Deelen P, et al. Unraveling the regulatory mechanisms underlying tissue-dependent genetic variation of gene expression. PLoS Genet 2012;8:e1002431.
22. Fehrmann RS, Jansen RC, Veldink JH, et al. Trans-eQTLs reveal that independent genetic variants associated with a complex phenotype converge on intermediate genes, with a major role for the HLA. PLoS Genet 2011;7:e1002197.
23. van de Sluis B, Muller P, Duran K, et al. Increased activity of hypoxia-inducible factor 1 is associated with early embryonic lethality in *Commd1* null mice. Mol Cell Biol 2007;27:4142–4156.
24. Vonk WI, Bartuzi P, de Bie P, et al. Liver-specific *Commd1* knockout mice are susceptible to hepatic copper accumulation. PLoS One 2011;6:e29183.
25. **Mao X, Gluck N**, Chen B, et al. Copper metabolism MURR1 domain containing 1 (COMMD1) regulates Cullin-RING ligases by preventing Cullin-associated NEDD8-dissociated (CAND1) binding. J Biol Chem 2011;286:32355–32365.
26. **Starokadomskyy P, Gluck N**, Li H, et al. CCDC22 deficiency in humans blunts activation of proinflammatory NF-κB signaling. J Clin Invest 2013;123:2244–2256.
27. Barish GD, Yu RT, Karunasiri M, et al. Bcl-6 and NF-κB cistromes mediate opposing regulation of the innate immune response. Genes Dev 2010;24:2760–2765.
28. Reveille JD, Sims AM, Danoy P, et al. Genome-wide association study of ankylosing spondylitis identifies non-MHC susceptibility loci. Nat Genet 2010;42:123–127.
29. **Okada Y, Terao C, Ikari K, Kochi Y**, et al. Meta-analysis identifies nine new loci associated with rheumatoid arthritis in the Japanese population. Nat Genet 2012;44:511–516.
30. Kenny EE, Pe'er I, Karban A, et al. A genome-wide scan of Ashkenazi Jewish Crohn's disease suggests novel susceptibility loci. PLoS Genet 2012;8:e1002559.
31. Anderson CA, Boucher G, Lees CW, et al. Meta-analysis identifies 29 additional ulcerative colitis risk loci, increasing the number of confirmed associations to 47. Nat Genet 2011;43:246–252.
32. **Franke A, McGovern DP, Barrett JC**, et al. Genome-wide meta-analysis increases to 71 the number of confirmed Crohn's disease susceptibility loci. Nat Genet 2010;42:1118–1125.
33. Consortium TEP. A user's guide to the encyclopedia of DNA elements (ENCODE). PLoS Biol 2011;9:e1001046.
34. **Kaikkonen MU, Spann NJ**, Heinz S, et al. Remodeling of the enhancer landscape during macrophage activation is coupled to enhancer transcription. Mol Cell 2013;51:310–325.
35. Nicolae DL, Gamazon E, Zhang W, et al. Trait-associated SNPs are more likely to be eQTLs: annotation to enhance discovery from GWAS. PLoS Genet 2010;6:e1000888.
36. Greten FR, Eckmann L, Greten TF, et al. IKKβ links inflammation and tumorigenesis in a mouse model of colitis-associated cancer. Cell 2004;118:285–296.
37. **Bollrath J, Phesse TJ**, von Burstin VA, et al. gp130-mediated Stat3 activation in enterocytes regulates cell survival and cell-cycle progression during colitis-associated tumorigenesis. Cancer Cell 2009;15:91–102.
38. Bollrath J, Greten FR. IKK/NF-κB and STAT3 pathways: central signalling hubs in inflammation-mediated tumour promotion and metastasis. EMBO Rep 2009;10:1314–1319.

39. **Weiss KH, Lozoya JC**, Tuma S, et al. Copper-induced translocation of the Wilson disease protein ATP7B independent of Murr1/COMMD1 and Rab7. Am J Pathol 2008;173:1783–1794.
40. **Miyayama T, Hiraoka D**, Kawaji F, et al. Roles of COMM-domain-containing 1 in stability and recruitment of the copper-transporting ATPase in a mouse hepatoma cell line. Biochem J 2010;429:53–61.
41. Chang T, Ke Y, Ly K, et al. COMMD1 regulates the delta epithelial sodium channel (δENaC) through trafficking and ubiquitination. Biochem Biophys Res Commun 2011; 411:506–511.
42. **Nenci A, Becker C**, Wullaert A, et al. Epithelial NEMO links innate immunity to chronic intestinal inflammation. Nature 2007;446:557–561.
43. Grivennikov SI, Greten FR, Karin M. Immunity, inflammation, and cancer. Cell 2010;140:883–899.
44. Popivanova BK, Kitamura K, Wu Y, et al. Blocking TNF-α in mice reduces colorectal carcinogenesis associated with chronic colitis. J Clin Invest 2008;118:560–570.
45. Kabakchiev B, Silverberg MS. Expression quantitative trait loci analysis identifies associations between genotype and gene expression in human intestine. Gastroenterology 2013;144:1488–1496. 1496 e1–3.
46. Rivas MA, Beaudoin M, Gardet A, et al. Deep resequencing of GWAS loci identifies independent rare variants associated with inflammatory bowel disease. Nat Genet 2011;43:1066–1073.

Author names in bold designate shared co-first authorship.

Received December 11, 2013. Accepted April 5, 2014.

Reprint requests
Address requests for reprints to: Ezra Burstein, MD, PhD, Departments of Internal Medicine and Molecular Biology, University of Texas Southwestern Medical Center, 5323 Harry Hines Boulevard, Dallas, Texas 75230-9151. e-mail: ezra.burstein@utsouthwestern.edu; fax: (214) 648-2022.

Acknowledgments
The authors are grateful to Eric Fearon for kindly providing some of the reagents used here. The authors are also grateful to John Shelton, Christine Komarck, and Baozhi Chen for technical support for this project.

Conflicts of interest
The authors disclose no conflicts.

Funding
Supported by a National Institutes of Health grant (R01 DK073639 to E.B.), a CCFA Senior Research Award (SRA 2737 to E.B.), a Cancer Prevention and Research Institute of Texas grant (CPRIT RP130409 to E.B.), the Disease Oriented Clinical Scholars' Program at University of Texas Southwestern (E.B.), a VIDI grant (91713308 to R.K.W.) from The Netherlands Organization for Scientific Research, a start-up grant from the US–Israel Binational Science Foundation (BSF 2009339 to N.G.), a grant from the German Israeli Foundation (N.G.), and funding provided to the Estonian Genome Center at the University of Tartu (T.E. and A.M.) in the form of FP7 programs (ENGAGE, OPENGENE), targeted financing from the Estonian Government (SF0180142s08), Estonian Research Roadmap through the Estonian Ministry of Education and Research, Center of Excellence in Genomics (EXCEGEN), and the University of Tartu (SP1GVARENG).

Supplementary Materials and Methods

Mouse Strains

Mice were housed in barrier facilities and fed an irradiated standard diet. All animal procedures were approved by the Care and Use Committee. The conditional *Commd1* allele recently was described.[1] LysM-Cre knock-in mice were obtained from the Jackson Laboratory (Bar Harbor, ME). Villin-Cre mice kindly were provided by Dr Eric Fearon.

Sepsis Models

Cecal ligation and puncture was performed as previously described.[2] Overall, the surgical time was kept to fewer than 15–20 minutes. After surgery, the mice were housed individually and monitored in a blinded manner (ie, without knowledge of the specific genotypes). This was performed every hour for the first 4–6 hours, then every 2 hours for the next 6 hours, and, finally, every 4–6 hours until the conclusion of the experiment or the need for euthanasia arose (based on morbidity criteria) (Supplementary Table 5). For the LPS model, LPS (*Escherichia coli* 055:B5; Sigma, St. Louis, MO) was diluted in water to 0.2 mg/mL and placed in a water bath sonicator (model FS20; Fisher, Waltham, MA) for 15–30 minutes at room temperature before use. After sonication, the LPS was filtered (0.2-μm pore) and injected intraperitoneally (0.1 mg/mouse). After injection, the mice were monitored similarly for morbidity until the conclusion of the experiment (Supplementary Table 5). Bacterial cultures were performed as previously described[3] and tissue RNA was extracted as noted later. Blood also was collected through orbital puncture, and plasma was separated using EDTA (5 mmol/L).

Acute and Chronic DSS-Induced Colitis

For the acute colitis model, DSS (Fisher) was administered in the drinking water at a concentration of 3 g/dL (3%). Freshly prepared DSS drinking solution was replaced every 5 days. Mice were housed in individual cages and evaluated daily for their weight and the presence of diarrhea or bleeding to calculate a disease activity index (Supplementary Table 6), which was based on the scoring system reported by Cooper et al.[4] Evaluation for occult bleeding included Hemoccult testing (Beckman Coulter, Brea, CA). Treatment was given for up to 10 days and animals showing severe distress were euthanized at any point during the experiment.

For the chronic colitis and cancer model, the animals were given azoxymethane intraperitoneally (10 mg/kg; Sigma). After 7 days, DSS was given in the drinking water over 4 days at a concentration of 2.5% followed by 10 days of regular water. This was repeated for 3 cycles and at the end of 7 or 10 weeks, the animals were euthanized, and the spleen and colon were harvested. The organ length and weight were determined and the colon was opened along the mesenteric side, and tumors were counted using a dissecting microscope (Zeiss Stemi 2000-C, Jena, Germany). Tumor volumes were calculated using the following formula: (width^2) $\times$ (height/2).

Histology and Immunohistochemistry

At the time of euthanasia, the colon was dissected and opened along the mesenteric side. The open colon was transected longitudinally with one half rolled onto itself as a Swiss roll and fixed in 4% paraformaldehyde (in phosphate-buffered saline). After paraffin embedding and sectioning, the tissue was stained with H&E. The second half was used for RNA extraction as described later. A histologic severity index[4] was used to score colonic sections from mice with acute DSS colitis (Supplementary Table 7). In chronic colitis/dysplasia models (azoxymethane/DSS at 7 weeks), Swiss-roll sections of the colon were assessed for the presence of architectural distortion, dysplasia, multifocal dysplasia, or high-grade dysplasia according to standard clinical pathology criteria. The number of individual foci was not quantitated by this approach. All histopathologic analyses were performed in a blinded fashion by a gastrointestinal pathologist (S.D.M.). For CD68 staining, a tissue microarray was generated using random colonic tissue cores obtained from blocks previously prepared from mice with acute colitis. After constructing the microarrays, 5-μm sections were subjected to CD68 staining (clone F8–11; Biolegend, San Diego, CA). Staining was performed on a Ventana Benchmark XT Automated IHC Stainer with Mild CC1 (Cell Conditioning 1) and 32 minutes of primary antibody incubation at a 1:25 dilution (in Chemmate Ab diluent, Dako, Carpinteria, CA). The detection was performed with an Ultraview Universal DAB detection Kit (cat. 760–500; Ventana, Tucson, AZ). The slides were counterstained with Mayer's hematoxylin. Images then were analyzed using ImageJ software (National Institutes of Health, Bethesda, MD) and cell counts were normalized to the surface area using the surface of a microscopic field as a reference. Co-staining for COMMD1[5] and F4/80 (11–4801; eBioscience, San Diego, CA) was performed using frozen sections of mouse colon tissue embedded in optimum cutting temperature compound using a previously reported protocol.

Multiplex Cytokine Measurements

EDTA plasma was separated from blood samples by centrifugation and stored at -80°C. Full-thickness colonic tissue (1 cm of rectum) was harvested form colitic mice and cultured in a 12-well cell culture dish with 1 mL of complete Dulbecco's modified Eagle medium culture media. The supernatant was collected 24 hours later, centrifuged, and stored at -80°C until measurement. Cytokine measurements were performed using Milliplex MAP beads (Millipore, Billerica, MA) and run on a Luminex Magpix with the Luminex xPONENT software (Luminex, Austin, TX). Data analysis was performed using Milliplex Analyst.

Cell Isolation and Cell Culture

The generation and immortalization of mouse embryo fibroblasts from the *Commd1* floxed mouse has been reported previously.[6] These cells were maintained in high-glucose Dulbecco's modified Eagle medium containing 10% fetal calf serum and treated with MG-132 (20 μmol/L for 3 h) for precipitation of ubiquitinated RelA, as described

later. BMDMs were generated by isolation of bone marrow cells from long bones, which were cultured in Roswell Park Memorial Institute (RPMI) media supplemented with 10% fetal calf serum, antibiotics (100 μg/mL penicillin G and 100 μg/mL streptomycin), and Fungizone (Fisher), in the presence of granulocyte-macrophage colony–stimulating factor (20 ng/mL; Peprotech, Rocky Hill, NJ). Myeloid differentiation was allowed to proceed for 10 days. In specific experiments, cells were treated with LPS (10 ng/mL, *E coli* 026:B6; Sigma). Hypoxia conditions (3% oxygen) were established in HeraCell incubators (ThermoFisher scientific, Waltham, MA). Splenocytes, thymocytes, or mesenteric lymph node cells were isolated according to standard protocols. Briefly, after removing the respective organs and placing them on a sterile dish containing RPMI, the tissue manually was ground and strained through a 40-μm tissue strainer. After centrifugation (300*g* for 5 minutes at 4°C), the cell pellet was resuspended in 2 mL of Ammonium-Chloride-Potassium buffer (150 mmol/L NH_4Cl, 10 mmol/L $KHCO_3$, 0.1 mmol/L EDTA, pH^+ 7.2) to lyze red blood cells. After 3 minutes at room temperature, the ACK lysis was neutralized by adding 10 mL of fluorescence-activated cell sorter media buffer (0.01% sodium azide, 2.5% fetal calf serum in phosphate-buffered saline). This cell suspension was strained again through the tissue strainer to obtain a single-cell suspension, which was pelleted by centrifugation. Gastrointestinal epithelial cells were isolated according to a previously described method.[7] Briefly, the entire colon, small bowel, or stomach was harvested and flushed clean with 1 mmol/L dithiothreitol in Krebs–Ringer bicarbonate buffer (10 mmol/L D-glucose, 0.5 mmol/L $MgCl_2$, 4.6 mmol/L KCl, 120 mmol/L NaCl, 0.7 mmol/L Na_2HPO_4, 1.5 mmol/L NaH_2PO_4, 15 mmol/L $NaHCO_3$). The lumen was filled with Krebs–Ringer bicarbonate buffer supplemented with 10 mmol/L EDTA and 1 mmol/L dithiothreitol, and both ends were ligated. The ligated colon was placed in a 50-mL conical tube with 30 mL of Krebs–Ringer bicarbonate buffer and placed at 37°C for 20 minutes with agitation. The sealed intestinal segment was palpated gently to loosen the cells, then cut on one end to drain the contents into a 1.7-mL microfuge tube. The cells were collected by centrifugation at 300*g* for 5 minutes and rinsed once with Krebs–Ringer bicarbonate buffer.

Flow Cytometry

Cells were resuspended in 2 mL of fluorescence-activated cell sorter media buffer and the cells from the mesenteric lymph node were resuspended in 600 μL. For antibody staining, 100 μL of each cell suspension was incubated on ice with the following primary antibodies: anti-B220-PE (BD Pharmingen, San Jose, CA), anti-CD3–PE (BD Pharmingen), anti-CD4–perCP (BD Pharmingen), anti-CD8a–APC (BD Pharmingen), anti-Ly6G–APC (eBioscience), anti-Ly6C–PerCP-Cy5.5 (eBioscience), anti-CD11C–APC (BD Pharmingen), anti-CD11b–PE (eBioscience), anti-F4/80–fluorescein isothiocyanate (eBioscience), and corresponding isotype controls. After 30 minutes, the cells were pelleted by centrifugation (300*g* for 5 minutes at 4°C) and washed twice in 500 μL of fluorescence-activated cell sorter media buffer. Flow cytometric analysis was performed using FACSCalibur (BD Biosciences, Mountain View, CA) and analyzed using FlowJo software (version 7.6.5, FlowJo, Ashland, OR).

Protein Extraction, Immunoblotting, and Immunoprecipitation

Cell lysate preparation, nuclear extract preparation, immunoprecipitation, denatured immunoprecipitation, and immunoblotting were performed as previously described.[5,8,9] Protein lysates from mouse tissues were prepared after snap freezing the samples in liquid nitrogen. After mincing with a razor blade, tissue pieces were submerged in lysis buffer (50 mmol/L Tris-Hcl, pH^+ 7.5, 250 mmol/L NaCl, 3 mmol/L EDTA, 3 mmol/L ethylene glycol-bis(β-aminoethyl ether)-*N,N,N′,N′*-tetraacetic acid, 1% Triton X-100, 0.5% NP40, 10% glycerol, and 25 mmol/L Na-pyrophosphate) supplemented with protease inhibitor tablets (Roche, San Francisco, CA). Thereafter, tissue homogenization was performed using a 2-mL Douncer and a cleared lysate (supernatant after 10,000*g* centrifugation) was used for further analysis. The following antibodies were used for Western blotting in this study: β-actin (A5441; Sigma), COMMD1,[5] COMMD9,[10] IκB-α (06–494; Upstate Biotechnologies, Billerica, MA), phosphor-IκB-α (9246; Cell Signaling, Danvers, MA), RelA (sc-372 and sc-8008; Santa Cruz Biotechnology, Santa Cruz, CA), and ubiquitin (3936; Cell Signaling).

RNA Extraction and Quantitative Real-Time Reverse-Transcription Polymerase Chain Reaction

In most cases, RNA was extracted using TRIzol (Invitrogen, Grand Island, NY) according to the manufacturer's instructions. In the case of colonic RNA from colitic mice, we obtained better results by first stabilizing the freshly isolated tissue in RNAlater (Qiagen, Hilden, Germany), followed by RNA extraction using the RNeasy chromatography method (Qiagen), according to the manufacturer's instructions. RNA (5 μg) was used for complementary DNA synthesis using the Superscript III strand synthesis system (Invitrogen). Real-time polymerase chain reaction was performed in an Eppendorf real-time polymerase chain reaction system. In most cases, SYBR Green–based detection (Invitrogen) was used using gene-specific primers, as noted in Supplementary Table 8. Experiments were performed in triplicate, data were normalized to housekeeping genes, and the relative abundance of transcripts was calculated by the comparative $\Delta\Delta Ct$ method.

Microarray Analysis

The primary data for this analysis are available in the Gene Expression Omnibus database at National Center for Biotechnology Information (NCBI, Accession GSE53368). The Whole Mouse Genome Oligo Microarray V2 (G4846A, ID 026655; Agilent Technologies, Santa Clara, CA) used in this study contains 44,397 oligonucleotide probes covering the

entire murine transcriptome. Synthesis of Cy3-labeled complementary RNA was performed with the Quick Amp Labeling kit, one color (5190-0442; Agilent Technologies) according to the manufacturer's recommendations. Complementary RNA fragmentation, hybridization, and washing steps also were performed exactly as recommended per the One-Color Microarray-Based Gene Expression Analysis Protocol V5.7. Slides were scanned on the Agilent Micro Array Scanner G2565CA (pixel resolution, 5 μm; bit depth, 20). Data extraction was performed with the Feature Extraction Software V10.7.3.1 by using the recommended default extraction protocol file GE1_107_Sep09.xml. The single-channel data generated by the Feature Extraction software were normalized and analyzed in Genespring GX software, version 12.0 (Agilent Technologies). Low expression values were increased to the constant value 15 (defined as the threshold) to minimize false-positive ratios. Data were $\log_2$-transformed and normalized to the 75th percentile of each array according to the standard procedure in Genespring GX.

Only probes referring to transcripts of annotated genes were considered and Agilent probe annotation was used. In cases of multiple probes per gene the value from that probe with the highest arithmetic mean intensity across all 12 hybridizations was selected. Genes were considered as measurable when the arithmetic mean of (anti-$\log_2$–retransformed) intensity values calculated from all 12 samples was greater than 100 and the mean intensity in at least 1 of 6 averaged conditions was greater than 50. Entities showing technical impairments were excluded from analyses. By using these criteria, of 44,397 probes, 18,682 probes corresponding to 11,441 genes were selected for further analysis. Genes were considered as regulated by LPS or by Commd1 KO according to the following criteria: the fold-change of mean values in at least 1 of 3 ratios was greater than 3-fold and regulation was consistent with the same trend in each single (nonaveraged) comparison. The following ratios were calculated: Commd1 KO vs WT, LPS 3 hours WT vs WT, LPS 24 hours WT vs WT. In the resulting gene set Commd1-dependent genes were defined by at least 2-fold differences of the following ratios of mean intensity values: deregulated basal expression (ratio Commd1 KO vs WT), deregulated less than 3 hours LPS treatment (Commd1 KO LPS 3 h vs WT LPS 3 h), and deregulated less than 24 hours LPS treatment (Commd1 KO LPS 24 h vs WT LPS 24 h). The ratio values of the resulting COMMD1-dependent 225 genes were analyzed by hierarchical cluster analysis using MeV MultiExperimentViewer, version 4.8.1, 2011 (available: www.tm4.org) with cluster settings "average" as linkage method and "Manhattan distance" as distance measure.

Gene function analysis was performed using the DAVID (v6.7) software platform (maintained by National Institute of Allergy and Infectious Diseases and available at http://david.abcc.ncifcrf.gov/home.jsp). Functional annotation was performed using the KEGG database (KEGG Mapper v1.6, released October 1, 2013). The regulation of genes of interest by NF-κB was ascertained by comparing each gene to 2 partially redundant data sets: a curated database of published NF-κB gene targets (publicly available and maintained at www.NF-κB.org), and, second, a chromatin immunoprecipitation seq data set of RelA-regulated genes in LPS-stimulated BMDMs.[11]

References

1. Vonk WI, Bartuzi P, de Bie P, et al. Liver-specific *Commd1* knockout mice are susceptible to hepatic copper accumulation. PLoS One 2011;6:e29183.
2. Toscano MG, Ganea D, Gamero AM. Cecal ligation puncture procedure. J Vis Exp 2011;pii:2860.
3. Kirkland D, Benson A, Mirpuri J, et al. B cell-intrinsic MyD88 signaling prevents the lethal dissemination of commensal bacteria during colonic damage. Immunity 2012;36:228–238.
4. Cooper HS, Murthy SN, Shah RS, et al. Clinicopathologic study of dextran sulfate sodium experimental murine colitis. Lab Invest 1993;69:238–249.
5. Burstein E, Hoberg JE, Wilkinson AS, et al. COMMD proteins: a novel family of structural and functional homologs of MURR1. J Biol Chem 2005;280:22222–22232.
6. Vonk WI, de Bie P, Wichers CG, et al. The copper-transporting capacity of ATP7A mutants associated with Menkes disease is ameliorated by COMMD1 as a result of improved protein expression. Cell Mol Life Sci 2012;69:149–163.
7. Ahnen DJ, Reed TA, Bozdech JM. Isolation and characterization of populations of mature and immature rat colonocytes. Am J Physiol 1988;254:G610–G621.
8. Burstein E, Ganesh L, Dick RD, et al. A novel role for XIAP in copper homeostasis through regulation of MURR1. EMBO J 2004;23:244–254.
9. Mao X, Gluck N, Li D, et al. GCN5 is a required cofactor for a ubiquitin ligase that targets NF-κB/RelA. Genes Dev 2009;23:849–861.
10. Starokadomskyy P, Gluck N, Li H, et al. CCDC22 deficiency in humans blunts activation of proinflammatory NF-κB signaling. J Clin Invest 2013;123:2244–2256.
11. Barish GD, Yu RT, Karunasiri M, et al. Bcl-6 and NF-κB cistromes mediate opposing regulation of the innate immune response. Genes Dev 2010;24:2760–2765.